Available online at www.sciencedirect.com
SCIENCE DIRECT
Journal of Molecular Spectroscopy 236 (2006) 178–188
Journal of MOLECULAR SPECTROSCOPY
www.elsevier.com/locate/jms

On the $X^2\Sigma^+$, $A^2\Pi$, and $C^2\Sigma^+$ states of BeH, BeD, and BeT

Robert J. Le Roy [a,*], Dominique R.T. Appadoo [a], Reginald Colin [b], Peter F. Bernath [a]

[a] Department of Chemistry, University of Waterloo, Waterloo, Ont., Canada N2L 3G1
[b] Laboratoire de Chimie Quantique et Photophysique, Université Libre de Bruxelles, C.P. 160/09, 50 av. F.D. Roosevelt, 1050 Brussels, Belgium

Received 26 November 2005; in revised form 21 January 2006
Available online 10 March 2006

Abstract

New Fourier transform measurements for the $A^2\Pi - X^2\Sigma^+$ system of BeH are combined with previously published $A - X$ data for BeH, BeD, and BeT, with existing data for the $C^2\Sigma^+ - X^2\Sigma^+$ system, and with recent vibration–rotation data for BeH and BeD, and fitted using combined-isotopologue Dunham expansion and direct-potential-fit methods. This data set provides direct spectroscopic information spanning 95% of the ground $X^2\Sigma^+$ state potential well, and provides the most comprehensive spectroscopic description of this state reported to date. The analysis of this data set allows us to study the breakdown of the Born–Oppenheimer approximation for a metal hydride from the minimum of the potential well to near the dissociation limit. Improved molecular constants are also determined for the $A^2\Pi$ and $C^2\Sigma^+$ states.

Keywords: Metal hydride; Born–Oppenheimer breakdown; Fourier transform emission spectroscopy; BeH; Direct Potential fit

1. Introduction

The BeH molecule and its isotopologues BeD and BeT have been the subject of a number of spectroscopic investigations. The most recent studies used high resolution Fourier transform (FT) spectrometers to examine the infrared (IR) spectra [1] and the $\Delta v = 0$ sequences of the $A^2\Pi - X^2\Sigma^+$ transition [2,3] of both BeH and BeD. Earlier literature reported measurements performed with plate spectrographs of the $\Delta v = 0$ and -1 sequences of the $A^2\Pi - X^2\Sigma^+$ system for BeH and BeD [4,5], of the 0–0, 1–1, 2–2, and 3–3 bands of the same transition in BeT [6], and of several bands of the $C^2\Sigma^+ - X^2\Sigma^+$ systems of BeH and BeD [4]. Absorption spectra involving Rydberg states have also been analyzed [7,8].

With only five electrons, the beryllium monohydride molecule has been the target of many ab initio calculations [9–18], and is often used to test new methods for open-shell systems. The availability of information for three isotopologues and its small reduced mass also make beryllium monohydride an interesting species for examining Born–Oppenheimer breakdown (BOB) effects. Since the available spectroscopic information covers 95% of the ground state potential well, the BeH molecule is also very well suited for the empirical determination of a potential energy curve using direct-potential-fit procedures [19–22].

Shayesteh et al. [1] reported a combined-isotopologue analysis of the IR data for BeH and BeD which yielded well defined Dunham constants and BOB parameters for the ground state. However, the fact that their data set was limited to the range $v'' \leqslant 4$ while the vibrational polynomial orders used for G_v, B_v and the associated BOB terms were all also equal to 4 means that the physical significance of some of those BOB parameters may be affected by model-dependence or interparameter correlation. The other modern experimental studies of this system preceded the availability of the new IR data [1], and treated BeH and BeD as independent species [2,3]. A central objective of the present paper is therefore to use all available data to obtain optimal Dunham constants and BOB parameters, and to determine the best possible potential energy curve for the $X^2\Sigma^+$ ground state.

It has been shown previously that the $C^2\Sigma^+$ and $A^2\Pi$ states of BeH interact strongly [4], so all previous analyses

* Corresponding author. Fax: +1 519 746 0435.
E-mail address: leroy@uwaterloo.ca (R.J. Le Roy).

0022-2852/$ - see front matter © 2006 Elsevier Inc. All rights reserved.
doi:10.1016/j.jms.2006.01.010

of the $A - X$ and $C - X$ systems omitted perturbed lines from the final fits. Unfortunately, the identification of perturbed lines is somewhat subjective, and the ground-state constants obtained in this way will have been affected by the choice of omitted lines. This paper uses an alternate approach in which the Dunham expansion coefficients or parameterized potential function model for the ground state are determined in analyses in which all excited-state rovibrational levels are represented by individual term values. The properties of the ground state determined in this way cannot be affected by the choice of which lines are identified as being perturbed, and hence omitted from the analysis, or of which model is used to represent the perturbed levels of the $A^2\Pi$ and $C^2\Sigma^+$ states. The only disadvantage of this approach is the fact that since the upper-state level energies are not linked directly to one another by any model, only transitions involving excited-state levels with transitions into two or more ground-state levels can be used in the fit. In the present case, this significantly reduces the number of transitions which provide information on the ground state.

In the final stage of our analysis, with the ground-state properties defined by the analysis described above, the full electronic transition data set is used to determine improved descriptions of the $A^2\Pi$ and $C^2\Sigma^+$ states.

2. Overview of the data

At the same time that the vibration–rotation spectra of BeH and BeD were recorded [1], some new FT spectra of the $A - X$ system of BeH were obtained. These new $A - X$ spectra contained the 0–1, 1–2, and 2–3 bands, and were calibrated on the same wavenumber scale as the $\Delta v = 0$ bands reported in our 1998 paper [2]. These new BeH bands were then used to re-calibrate the old $\Delta v = -1$ bands which had been measured with a grating spectrograph [4]. The data used in our analysis, together with the range of vibrational levels observed and the associated uncertainties, are summarized in Table 1.

Our global electronic and IR data set for the three isotopologues consisted of some 3496 transitions, and the uncertainties initially assigned to the different data subsets were based on values reported in the respective source publications. Generally, data recorded on photographic plates were assigned uncertainties of 0.1 cm^{-1}, FT visible data 0.01 cm^{-1}, and FTIR data 0.001 cm^{-1}. Upon further inspection of the data, some 365 blended lines were identified, mainly in the lower resolution plate measurements and the weaker FT bands; their uncertainties were increased by a factor of 2 relative to the standard uncertainties assigned to that particular data source. In addition, 155 other transitions were removed when they were found to be statistical outliers with discrepancies from our optimized models of more that eight times their estimated uncertainties.

Removal of the outliers left us with a total of some 3341 data. However, as was pointed out in the Introduction, our determination of the properties of the ground state is based on an analysis in which all $A^2\Pi$ and $C^2\Sigma^+$ energy levels are represented by independent term values; this means that data originating in the 520 excited-state levels which were coupled to only one ground-state level do not provide any information about ground-state properties. As a result, the data set used to determine the $X^2\Sigma^+$ state parameters and potential function consists of a total of 2821 transitions.

Fig. 1 shows the complete set of observed levels for the ground state of BeH, BeD, and BeT, plotted on a mass-reduced scale which makes the rotational energies for the different isotopologues equivalent. We note that for the ground state of BeH, the data set covers all vibrational levels from $v = 0$ to 10, and that all vibrational levels are connected. For BeD, however, no transitions involving the

Table 1
Overview of the data used in the present analysis

Species	Data type	# lines	Δv	v''-range	unc./cm^{-1}	Ref.
BeH	IR	97	1	0–1	0.001	[1]
		43	1	2	0.002	[1]
		24	1	3	0.003	[1]
	$C - X$	229	($v' = 0$–2)	6–10	0.10	[4]
	$A - X$	92	−1	5–7	0.20	[4]
		46	−1	4	0.10	[4]
		227	−1	1–3	0.010	Present
		175	0	5–6	0.020	Present
		655	0	0–4	0.010	Present
BeD	IR	111	1	0–1	0.001	[1]
		42	1	2	0.002	[1]
		25	1	3	0.003	[1]
	$C - X$	198	($v' = 0$)	8–12	0.10	[4]
	$A - X$	108	−1	5–6	0.20	[3]
		263	−1	1–4	0.10	[3]
		95	0	5–6	0.020	[3]
		723	0	0–4	0.010	[3]
BeT	$A - X$	349	0	0–3	0.10	[6]

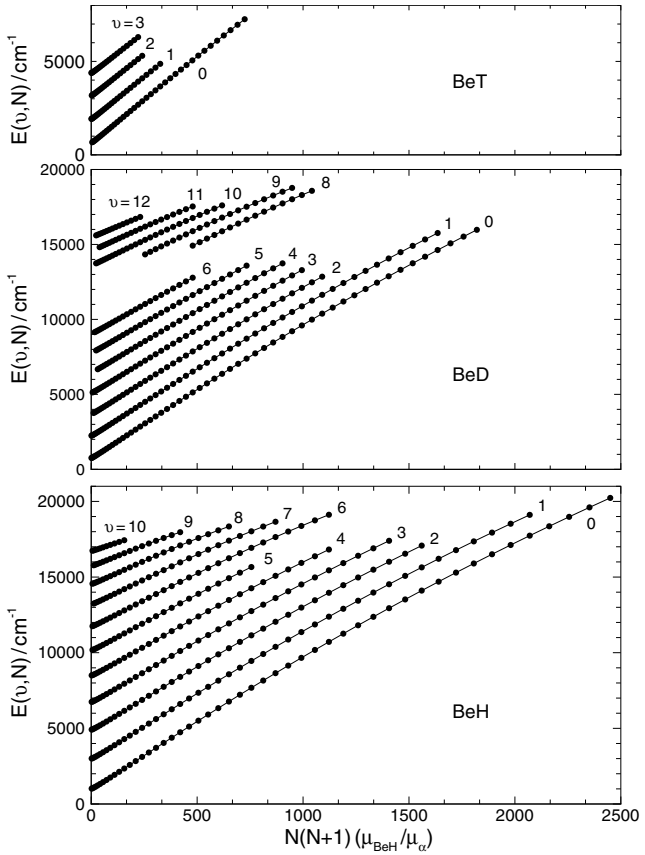

Fig. 1. Observed vibration–rotation levels in the $X^2\Sigma^+$ state of BeH, BeD, and BeT.

$v = 7$ level have been reported, and there are no transitions linking the levels $v \geqslant 8$ with those for $v \leqslant 6$. However, within a combined-isotopologue analysis of the data for the $X^2\Sigma^+$ state, those two blocks of levels are linked *via* data for BeH. For BeT, only the 0–0, 1–1, 2–2, and 3–3 $A^2\Pi - X^2\Sigma^+$ bands were observed, so the four ground-state vibrational levels are not linked to one another. Thus, while these data contribute to the overall behavior and determination of BOB effects in a global combined-isotopologue analysis, they cannot provide an independent description of BeT.

3. Analysis

In all of the fits described herein, each experimental datum $y_i^{\rm obs}$ was weighted by the inverse square of its estimated uncertainty u_i (see Table 1), and the overall quality of fit represented by the dimensionless root mean square deviation

$$\overline{dd} = \sqrt{\frac{1}{N}\sum_i^N [(y_i^{\rm calc} - y_i^{\rm obs})/u_i]^2}. \qquad (1)$$

In treatments of the $X^2\Sigma^+$ state, the spectroscopic data for BeH, BeD, and BeT were all fitted simultaneously.

3.1. Parameter-fit analysis of the ground $X^2\Sigma^+$ state

Although its highest-energy vibration–rotation levels present some challenges, the ground $X^2\Sigma^+$ state of BeH is generally well behaved, and its level energies may be accurately described by a generalized version of the familiar Dunham double power-series expansion in the vibrational (v) and rotational (J) quantum numbers. In this approach, the level energies for all isotopologues are represented by a common expression involving a single set of Dunham $Y_{l,m}$ coefficients and a (usually) modest number of BOB parameters. The present work used the formulation of [20], in which the vibration–rotation energies for isotopologue α in a Σ electronic state are written as

$$\begin{aligned} E_{v,J}^{(\alpha)} &= \sum_{m=0}^{m_{\max}} \sum_{l=0}^{l_{\max}(m)} Y_{l,m}^{(\alpha)} \left(v+\tfrac{1}{2}\right)^l [J(J+1)]^m \qquad (2) \\ &= \sum_{m=0}^{m_{\max}} \sum_{l=0}^{l_{\max}(m)} \left(\frac{\mu_1}{\mu_\alpha}\right)^{m+l/2} \left\{ Y_{l,m}^{(1)} + \frac{\Delta M_A^{(\alpha)}}{M_A^{(\alpha)}} \delta_{l,m}^A + \frac{\Delta M_B^{(\alpha)}}{M_B^{(\alpha)}} \delta_{l,m}^B \right\} \\ &\quad \left(v+\frac{1}{2}\right)^l [J(J+1)]^m \end{aligned}$$

in which $Y_{l,m}^{(1)}$ are the standard Dunham parameters for the chosen reference isotopologue ($\alpha = 1$), here BeH, $M_A^{(\alpha)}$ is the mass of atom A in isotopologue α, μ_α the normal reduced mass of that isotopologue, and $\Delta M_A^{(\alpha)} = M_A^{(\alpha)} - M_A^{(1)}$ the difference between the masses of atom A in isotopologue α and the chosen reference isotopologue.

The BOB coefficients $\delta_{l,m}^{A/B}$ appearing in Eq. (2) may only be determined in a combined analysis of data for two or more isotopologues. Since Be has only one stable isotope, the only BOB parameters that may be determined here are $\delta_{l,m}^{\rm H}$, so the conventional Dunham coefficients for the 'minor' isotopologues BeD and BeT are defined as

$$Y_{l,m}^{(\alpha)} = \left(\frac{\mu_{\rm BeH}}{\mu_\alpha}\right)^{m+l/2} \left\{ Y_{l,m}^{({\rm BeH})} + \frac{\Delta M_{\rm H}^{(\alpha)}}{M_{\rm H}^{(\alpha)}} \delta_{l,m}^{\rm H} \right\}. \qquad (3)$$

In principle, each rotational level of a $^2\Sigma^+$ state is split by spin–rotation interactions into e and f components [23], and such effects could readily be taken into account [24]. However, for the ground state of BeH those splittings were not resolved in the existing experiments. The "parameter-fit" analysis reported herein was performed using program DPARFIT [24].

After considerable experimentation, it was concluded that an optimal Dunham-type description of the $X^2\Sigma^+$ state was obtained with $m_{\max} = 6$ and $l_{\max}(m) = \{8,7,9,7,6,1,0\}$ for the $Y_{l,m}^{({\rm BeH})}$ coefficients and $l_{\max}(m) = \{3,1,0,0\}$ for the $\delta_{l,m}^{\rm H}$ BOB coefficients. Together with 941 $A^2\Pi$ and $C^2\Sigma^+$ state term values, these 51 molecular parameters yield a quality of fit indicated by $\overline{dd} = 1.01$; i.e., on average, the predictions of the model agree with experiment to within 1.01 times the estimated experimental uncertainties. The resulting parameter values are presented in Table 2, together with the 95% confidence

Table 2
Recommended Dunham-type parameter set describing the $X^2\Sigma^+$ state of BeH, BeD, and BeT, all with units cm^{-1}; for this fit, $\overline{dd} = 1.01$

Constant	BeH	BeD	BeT
$Y_{1,0}$	2061.2353 (290)	1529.9859899	1305.9833557
$Y_{2,0}$	−37.32666 (4400)	−20.5569917	−14.9761535
$10^3 Y_{3,0}$	84. (33)	34.84492	21.77332
$10^3 Y_{4,0}$	−118.63 (1400)	−35.96866	−19.0877805
$10^3 Y_{5,0}$	26.34 (350)	5.9262223	2.68421251
$10^3 Y_{6,0}$	−4.44983 (48000)	−0.74291311	−0.287200222
$10^6 Y_{7,0}$	360. (34)	44.5994532	14.7158068
$10^6 Y_{8,0}$	−12.971 (980)	−1.19243009	−0.33581127
$Y_{0,1}$	10.319921 (98)	5.6883043	4.145197495
$Y_{1,1}$	−0.3084176 (3600)	−0.126102209	−0.0784226052
$10^6 Y_{2,1}$	500. (500)	151.6002	80.4509
$10^6 Y_{3,1}$	−1137.3 (3200)	−255.88051	−115.89806
$10^6 Y_{4,1}$	357. (110)	59.602272	23.041437
$10^6 Y_{5,1}$	−87.186 (1900)	−10.8012442	−3.5639231
$10^6 Y_{6,1}$	9.5 (16)	0.87333944	0.2459492
$10^9 Y_{7,1}$	−433.2 (540)	−29.551556	−7.1031416
$10^6 Y_{0,2}$	−1033.88 (54)	−314.434724	−167.033465
$10^6 Y_{1,2}$	15.543 (2000)	3.4970111	1.58393
$10^6 Y_{2,2}$	−5.75 (290)	−0.9599806	−0.37111559
$10^6 Y_{3,2}$	3.522 (2000)	0.43633132	0.143969643
$10^9 Y_{4,2}$	−1222.2 (8000)	−112.357417	−31.6420113
$10^9 Y_{5,2}$	60. (210)	4.0930132	0.9838146
$10^9 Y_{6,2}$	60. (36)	3.03721533	0.6230939
$10^{12} Y_{7,2}$	−15088.53 (400000)	−566.76588	−99.240606
$10^{12} Y_{8,2}$	1384.62 (25000)	38.5940007	5.7678413
$10^{12} Y_{9,2}$	−45.4 (66)	−0.93902572	−0.119778475
$10^9 Y_{0,3}$	105.683 (10000)	17.735863	6.8682478
$10^9 Y_{1,3}$	−7.66 (330)	−0.9489773	−0.31311967
$10^9 Y_{2,3}$	9.4 (43)	0.86414639	0.24336026
$10^9 Y_{3,3}$	−9.1811 (26000)	−0.62630607	−0.150541675
$10^{12} Y_{4,3}$	4255.12 (83000)	215.395262	44.1889889
$10^{12} Y_{5,3}$	−995.1 (1400)	−37.3786397	−6.54499325
$10^{12} Y_{6,3}$	110.7 (110)	3.08558007	0.461137375
$10^{15} Y_{7,3}$	−4570. (350)	−94.523073	−12.0569963
$10^{12} Y_{0,4}$	−15.644 (800)	−1.4381602	−0.4050136
$10^{15} Y_{1,4}$	−300. (1700)	−20.46507	−4.91907
$10^{15} Y_{2,4}$	0.0 (21000)	0.0	0.0
$10^{15} Y_{3,4}$	730. (1200)	27.420769	4.801372
$10^{15} Y_{4,4}$	−537. (330)	−14.96799	−2.2369537
$10^{15} Y_{5,4}$	125.88 (4300)	2.6036246	0.33210825
$10^{18} Y_{6,4}$	−10300. (2200)	−158.08523	−17.210773
$10^{18} Y_{0,5}$	2570. (340)	130.09406	26.689189
$10^{18} Y_{1,5}$	−410. (51)	−15.40071	−2.696661
$10^{21} Y_{0,6}$	−300. (58)	−8.362006	−1.249695
$\delta^H_{1,0}$	1.2109 (70)		
$\delta^H_{2,0}$	−0.013 (4)		
$\delta^H_{3,0}$	0.00256 (66)		
$10^3 \times \delta^H_{0,1}$	21.013 (91)		
$10^3 \times \delta^H_{1,1}$	−0.407 (11)		
$10^6 \times \delta^H_{0,2}$	−6.35 (29)		
$10^9 \times \delta^H_{0,3}$	−1.1 (2)		

The numbers in parentheses represent 95% confidence limit uncertainties in the last digits shown.

limit (two σ) uncertainties in the 51 fit parameters and the 'minor isotopologue' $Y_{l,m}$ values for BeD and BeT generated from Eq. (3). The numbers of significant digits shown for the fitting parameters were determined by the sequentially rounding and re-fitting procedure of [19], while the numbers of digits shown for the BeD and BeT parameters were determined by its 'sensitivity rounding' criterion [19]. For the convenience of the reader, sets of band constants $\{G_v, B_v, -D_v, H_v, \ldots\}$ generated from these Dunham-type parameters are presented in Supplementary material available from the authors or from the Journal's data archive [25]. As mentioned earlier, the absence both of data for the $v = 7$ level of BeD, and of a link between its $v \leqslant 6$ and $v \geqslant 8$ levels was not a problem, because the combined-isotopologue analysis uses the BeH data to bridge the gap.

Some readers may be puzzled about the sometimes quite high relative uncertainties and occasional rounded-to-zero values seen in the list of fitted $Y^{(BeH)}_{l,m}$ parameters in Table 2. However, this is to be expected whenever one uses high-order Dunham polynomial expansions for cases in which the vibrational levels span a very large fraction of the potential energy well. Although the resulting expressions represent the individual vibration–rotation level energies with very high precision, the interparameter correlation between the expansion coefficients can give rise to very large relative uncertainties in some of them. In spite of those uncertainties, the various polynomial orders could not be reduced further without compromising the overall quality of fit. These results remind us that at most, only a few of the lowest-order coefficients in this type of empirical expansion generally have any real physical significance, while the higher-order coefficients merely provide a (generally non-unique) empirical way of representing the level energies. From this viewpoint, it is arguable that there is little purpose in even reporting uncertainties for most of the parameters in Table 2, since the parameters themselves have little or no physical significance, and those uncertainties cannot be used without access to the full 992×992 correlation matrix for the fit.

In summary, the X-state Dunham-type parameters of Table 2 supersede those obtained from the previous separate analyses of the IR data [1] and of the electronic spectra [2,3]. Our new values of the leading Dunham and BOB coefficients for each rotational order are generally fairly similar to those presented in the earlier work. However, the leading vibrational energy expansion coefficients reported in [2], and the vibrational BOB parameters reported in [1] are notable exceptions to this generalization. The vibrational Dunham and BOB parameters from those previous analyses are compared with our current recommended results in Table 3. The differences between the present results (first column) and the vibrational coefficients obtained from the electronic spectra [2] (last column) largely reflect the importance of the recent FTIR data [1] and the influence of the BeD data in our multi-isotopologue analysis. However, the considerable differences between the present recommended vibrational BOB parameters (first column) and those of Shayesteh et al. [1] (third column) have a more subtle origin.

The data set used by Shayesteh et al. [1] consisted of only the $\Delta v = 1$ BeH and BeD infrared spectra for $v'' = 0$–3. Since only four vibrational spacings were

Table 3
Comparison of vibrational Dunham and BOB parameters for BeH obtained from various analyses

Constant	All data present[a]	Only IR data		Electronic data Focsa et al. [2]
		Present[b]	Shayesteh et al. [1]	
$Y_{1,0}$	2061.235 (±0.029)	2061.081 (±0.012)	2061.416 (± 0.003)	2068.86 (±1.03)
$Y_{2,0}$	−37.327 (±0.044)	−37.055 (±0.013)	−37.433 (± 0.002)	−46.15 (±1.3)
$Y_{3,0}$	0.084 (±0.033)	−0.151 (±0.007)	0.0325 (±0.0007)	4.98 (±0.74)
$Y_{4,0}$	−0.119 (±0.014)	−0.0079 (±0.0015)	−0.04784 (± 0.00008)	−1.61 (±0.23)
$Y_{5,0}$	0.0263 (±0.004)	−0.0032 (±0.00012)	—	0.289 (±0.042)
$\delta^{H}_{1,0}$	1.211 (±0.007)	1.224 (±0.008)	0.767 (±0.008)	—
$\delta^{H}_{2,0}$	−0.013 (±0.004)	−0.015 (±0.005)	0.418 (±0.008)	—
$\delta^{H}_{3,0}$	0.0026 (±0.0007)	0.0023 (±0.0009)	−0.1565 (±0.0034)	—
$\delta^{H}_{4,0}$	—	—	0.0198 (±0.0005)	—

[a] For compactness, only 5 of the 8 vibrational $Y_{l,0}$ coefficients from Table 2 are shown here.
[b] From a new fit to the data of [1] (see text).

observed for each isotopologue, it seemed reasonable to restrict the order of the polynomial used to represent the vibrational energies to being $\leqslant 4$. However, to simultaneously obtain good agreement for both BeH and BeD required a vibrational BOB polynomial of order four. Within the parameterization of Eqs. (2) and (3), that is equivalent to performing independent fits for the two isotopologues. However, that approach overlooked a key assumption underlying such combined-isotopologue treatments: namely, that the vibrational spacings for the 'minor isotopologue(s)' (here BeD) should primarily be thought of as additional "fractional–v" values for the reference species (here BeH).

For BeH and BeD, the existence of a total of eight observed vibrational spacings clearly allows the vibrational polynomial order to be greater than four. The second column of Table 3 shows the results of a new combined-isotopologue fit to the IR data alone, in which $l_{\max}(0) = 5$ for the $Y^{(\mathrm{BeH})}_{l,m}$ terms and 3 for the $\delta^{H}_{l,m}$. This fit also uses a total of eight parameters to represent the vibrational energies, but since the Dunham $Y_{l,0}$ polynomial order is distinctly greater than that for the BOB expansion in $\delta^{H}_{l,0}$, it treats the latter as defining an independent correction function, rather than merely providing an alternate way of representing the independent $Y_{l,0}$ coefficients for the minor isotopologue. It is noteworthy that the vibrational BOB parameters yielded by this alternate parameterization of the fit to the IR data alone (column 2) are essentially identical to those obtained from the present fit to the global data set which includes levels up to $v'' = 10$. This shows that the more traditional approach of restricting the number of vibrational $Y_{l,m}$ parameters to being no larger than the number of vibrational spacings observed for the major isotopologue compromised the significance of the vibrational BOB parameters of [1]. Prior to the present work it had never been clearly determined whether one of these two types of parameterization should really be preferred over the other.

The present global analysis in which the vibrational data spanned the interval $v(\mathrm{BeH}) = 0$–10 requires the use of an order-8 polynomial for the $Y^{(\mathrm{BeH})}_{l,m}$ terms, but only an order-3 polynomial for the $\delta^{H}_{l,m}$ (first column of Table 2). The resulting BOB parameters differ sharply from those of Shayesteh et al. [1] (third column), but are in good agreement with those obtained from the present fit to the IR data (column 2) which used $l_{\max}(0) = 5$ for the $Y^{(\mathrm{BeH})}_{l,m}$ terms and 3 for the $\delta^{H}_{l,m}$. This confirms the suggestion that in a combined-isotopologue analysis, one should not necessarily limit polynomial expansion orders to the maximum value appropriate for a corresponding single-isotopologue analysis. This statement is particularly relevant for hydrides. On a more general note, the fact that the differences between the parameters values obtained in the different analyses are generally much larger than the uncertainties implied by any given fit reaffirms the general truth that model-dependence is often the main source of physical uncertainty in parameters determined from an empirical data analysis.

3.2. Direct-potential-fit (DPF) analysis of the ground $X^2\Sigma^+$ state

The conventional Dunham parameters for each isotopologue (see Table 2) may be used in the familiar Rydberg–Klein–Rees (RKR) inversion procedure [26,27] to generate potential energy curves for each species. However, the resulting pointwise potentials are not the most convenient to work with, and the discrepancies between the first-order semiclassical basis of the RKR procedure and the exact quantal methods usually used for calculations utilizing such potentials can give rise to significant errors in calculated system properties, especially for hydrides and other species of small reduced mass. Moreover, empirical Dunham-type polynomial level-energy expression such as Eq. (2) are well known to be unable to provide realistic predictions outside the range of the data used in the analysis.

In view of the above, it is becoming increasingly common to perform data analyses using fully quantum mechanical direct-potential-fit methods. In this approach the observed level energy spacings are fitted directly to difference between eigenvalues obtained by solving the effective radial Schrödinger equation [28,29]

$$\left\{-\frac{\hbar^2}{2\mu_\alpha}\frac{d^2}{dr^2}+\left[V_{\rm ad}^{(1)}(r)+\Delta V_{\rm ad}^{(\alpha)}(r)\right]+\frac{\hbar^2 J(J+1)}{2\mu_\alpha r^2}\left[1+g^{(\alpha)}(r)\right]\right\}\psi_{v,J}(r)=E_{v,J}\psi_{v,J}(r) \quad (4)$$

in which $V_{\rm ad}^{(1)}(r)$ is the total internuclear potential for the selected reference isotopologue, $\Delta V_{\rm ad}^{(\alpha)}(r)$ is the *difference* between the effective adiabatic potential for isotopologue-α and that for the reference species ($\alpha=1$), and $g^{(\alpha)}(r)$ is the non-adiabatic centrifugal potential correction function for isotopologue-α. The main part of this second term is due to the J-dependent mixing of the electronic wavefunction of the state in question with those for other electronic states. This mixing causes non-mechanical shifts of the rotational energy levels whose magnitudes are characterized by the $g^{(\alpha)}(r)$ function.

Both $\Delta V_{\rm ad}^{(\alpha)}(r)$ and $g^{(\alpha)}(r)$ are written as a sum of two terms, one for each component atom, whose magnitudes are inversely proportional to the mass of the particular atomic isotope [20,28–32]. Since Be has only the one stable isotope, in the present case these functions may be written as [21,33]

$$\Delta V_{\rm ad}^{(\alpha)}(r)=\frac{\Delta M_{\rm H}^{(\alpha)}}{M_{\rm H}^{(\alpha)}}\tilde{S}_{\rm ad}^{\rm H}(r) \quad (5)$$

$$g^{(\alpha)}(r)=\tilde{R}_{\rm na}^{\rm Be}(r)+\frac{M_{\rm H}^{(1)}}{M_{\rm H}^{(\alpha)}}\tilde{R}_{\rm na}^{\rm H}(r). \quad (6)$$

As was true for the BOB parameters $\delta_{l,m}^{(\rm H)}$ discussed in the previous section, the "adiabatic" BOB radial function $\tilde{S}_{\rm ad}^{\rm H}(r)$ can only be determined from a simultaneous analysis of data for multiple isotopologues. In a DPF analysis, however, an overall centrifugal BOB radial function $g^{(\alpha)}(r)$ can be determined in an analysis of data for only a single isotopologue, although in that case it would represent a weighted linear combination of $\tilde{R}_{\rm na}^{\rm Be}(r)$ and $\tilde{R}_{\rm na}^{\rm H}(r)$. In the present case, however, we would in principle be able to determine these two functions separately, if they are sufficiently strong.

In the present study of the ground $X^2\Sigma^+$ state of BeH, the effective adiabatic potential for the reference isotopologue BeH was represented by the EMO$_p$ form

$$V_{{\rm EMO}_p}(r)=\mathfrak{D}_{\rm e}\left[1-{\rm e}^{-\beta(y_p)\cdot(r-r_{\rm e})}\right]^2, \quad (7)$$

where $\mathfrak{D}_{\rm e}$ is the well depth, $r_{\rm e}$ the equilibrium distance, and the exponent coefficient in Eq. (7) is expressed as a simple power series

$$\beta_{{\rm EMO}_p}=\sum_{i=0}^{N}\beta_i y_p^i, \quad (8)$$

which is an expansion in terms of a version of a generalized variable introduced by Šurkus [34]:

$$y_p=y_p(r)=\frac{r^p-r_{\rm e}^p}{r^p+r_{\rm e}^p}. \quad (9)$$

Previous work has shown that defining the exponent coefficient $\beta(r)$ as an expansion in the variable $y_p(r)$ for some appropriate small integer value of $p>1$ (say, $p=2$–4) greatly reduces the probability that the resulting potential function will exhibit non-physical behaviour (e.g., turn over) at distances outside the radial interval to which the data are sensitive [21,31,35]. For the same reason, it was found that it is also sometimes desirable to allow the polynomial in Eq. (8) to have a lower order in the short-range repulsive wall region than in the attractive outer well region. Thus, a particular type of EMO potential is identified by the label EMO$_p(N_{\rm S},N_{\rm L})$, where the polynomial order in Eq. (8) is $N=N_{\rm S}$ when $r<r_{\rm e}$ and $N=N_{\rm L}$ when $r\geqslant r_{\rm e}$. This does mean that when $N_{\rm S}\neq N_{\rm L}$, derivatives of the potential of order $\min\{N_{\rm S},N_{\rm L}\}+2$ will not be continuous at the one point $r=r_{\rm e}$; however, since $\min\{N_{\rm S},N_{\rm L}\}$ is typically $\geqslant 4$, this is not a serious deficiency.

Following the discussion of [21] and [31], the radial strength functions for the potential energy and centrifugal BOB corrections are written in the forms [32]:

$$\tilde{S}_{\rm ad}^{\rm H}(r)=\left[1-y_p(r)\right]\sum_{i=0}u_i^{\rm H}\left[y_p(r)\right]^i+u_\infty^{\rm H}y_p(r), \quad (10)$$

$$\tilde{R}_{\rm na}^{\rm Be/H}(r)=\left[1-y_{\rm p}(r)\right]\sum_{i=0}t_i^{\rm Be/H}\left[y_p(r)\right]^i+t_\infty^{\rm Be/H}y_p(r). \quad (11)$$

Use of these expressions allows the appropriate asymptotic values and differences in well depths for different isotopologues to be explicit parameters in the fit [21]. In particular, since we are treating the ground electronic state, and the zero of energy is defined as ground-state atoms separated at infinity, $u_\infty^{\rm H}=0$. The value of $u_0^{\rm H}$ therefore defines the difference between the well depths for the hydrogenic isotopologues: $\delta\mathfrak{D}_{\rm e}(X)=[\Delta M_{\rm H}^{(\alpha)}/M_{\rm H}^{(\alpha)}]u_0^{\rm H}$. With regard to $\tilde{R}_{\rm na}^{\rm Be/H}$, we follow the Watson convention [28,29] of constraining the centrifugal BOB functions $\tilde{R}_{\rm na}^{\rm Be/H}(r)$ to be zero at $r_{\rm e}$, and hence fix $t_0^{\rm Be/H}=0$. Similarly, the arguments of [21] indicate that those BOB functions must go to zero as $r\to\infty$, which means that $t_\infty^{\rm Be/H}=0$. Note that the integer p used to define the radial variables in Eqs. (10) and (11) need not be the same as that used for the potential function itself, but it is usually convenient to make them the same. Fortran code for generating these potential energy and BOB radial functions may be found in subroutine POTGEN which is part of the freely available radial Schrödinger solver package LEVEL [36]. The DPF analysis reported below was performed using program DPOTFIT [22].

After considerable experimentation, it was found that an optimum combined-isotopologue direct potential fit to the global data set, with the vibration–rotation levels of the $A^2\Pi$ and $C^2\Sigma^+$ states being represented by independent term values, was provided by an EMO$_3(5,9)$ potential function for the $X^2\Sigma^+$ state. Since Be has only one stable isotope, only the $\tilde{S}_{\rm ad}^{\rm H}(r)$ potential-energy BOB function can be determined, and as mentioned above, its asymptotic value is fixed at $u_\infty^{\rm H}=0.0$ [21]. In principle, a combined-isotopologue fit might be able to determine the value of $u_0^{\rm H}$, which would define the difference between the well depths

for BeH and BeD. In the present case, however, this quantity was found to be very poorly determined, with significantly differences (of 10–20 cm^{-1}) between values yielded by fits to slightly different models. Hence, this parameter was fixed at the value $u_0^H = 0$ in the final fits. The fact that the available data are unable to determine the difference between the potential function well depths for BeH and BeD should not be surprising, since such differences are expected to be of the order of only a few cm^{-1}, while the highest point at which vibrational data are available for *both* species is ~2000 cm^{-1} from dissociation. Although the data might in principle be able to determine both centrifugal BOB functions $\tilde{R}^H_{na}(r)$ and $\tilde{R}^{Be}_{na}(r)$, in practice they proved to be completely insensitive to the latter.

Our current recommended model for the $X^2\Sigma^+$ state of BeH consists of an $EMO_3(5,9)$ potential function with the BOB functions of Eqs. (10) and (11) being defined by polynomials of order five and three, respectively. The resulting potential energy and BOB function parameters are given in Table 4, while the potential function is shown in Fig. 2 and the associated BOB radial functions in Fig. 3. The final parameter values were obtained using the sequential rounding and re-fitting procedure of [19]. For both types of BOB functions, Fig. 3 also shows the radial functions and $\overline{dd}$ value for fits performed using different polynomial orders in Eqs. (10) and (11). A polynomial of order 4 for $\tilde{S}^H_{ad}(r)$ or of order 2 for $\tilde{R}^H_{na}(r)$ clearly give significantly poorer quality fits, while if we use polynomial orders of 6 and 4, respectively, the quality if fit does not improve significantly and some of the resulting parameter values have very large relative uncertainties. For the case of $\tilde{S}^H_{ad}(r)$, we note that the order 5 and 6 polynomials only begin to diverge from one another at distances past the out-

Table 4
Parameters defining the recommended potential energy and BOB radial functions for the $X^2\Sigma^+$ state of BeH; for this fit, $\overline{dd} = 1.12$

Form	EMO_3 (5,9)
$\mathfrak{D}_e/cm^{-1}$	17590.00 (±200)
r_e/Å	1.342394 (±0.0000012)
β_0	1.8019222 (±0.00021)
β_1	0.256007 (±0.00021)
β_2	0.352991 (±0.00046)
β_3	0.3476 (±0.0013)
β_4	0.2519 (±0.0015)
β_5	−0.0070 (±0.027)
β_6	9.6395 (±0.62)
β_7	−32.2 (±2.2)
β_8	47.9117 (±3.0)
β_9	−23.42 (±1.6)
u_1^H/cm^{-1}	137.88 (±0.45)
u_2^H/cm^{-1}	−45.01 (±0.37)
u_3^H/cm^{-1}	127.5 (±6.0)
u_4^H/cm^{-1}	−85. (±8.1)
u_5^H/cm^{-1}	−63. (±11.)
t_1^H	0.001211 (±0.000041)
t_2^H	0.00078 (±0.00021)
t_3^H	0.00273 (±0.00012)

Numbers in parentheses are 95% confidence limit uncertainties, while the uncertainty given for $\mathfrak{D}_e$ is an ad hoc estimate, as discussed in the text.

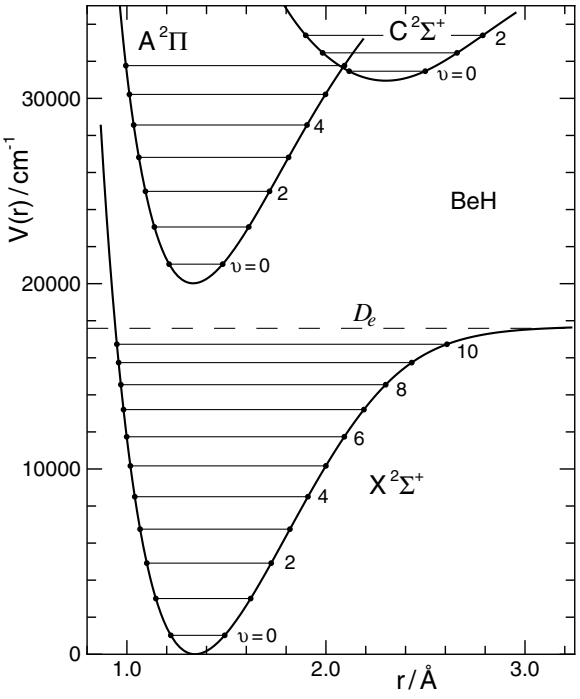

Fig. 2. Recommended $EMO_3(5,9)$ potential for the $X^2\Sigma^+$ of BeH, and RKR potentials for the $A^2\Pi$ and $C^2\Sigma^+$ states generated from the constants in Table 9, with the energies of the observed vibrational levels of the BeH isotopologue shown as horizontal lines.

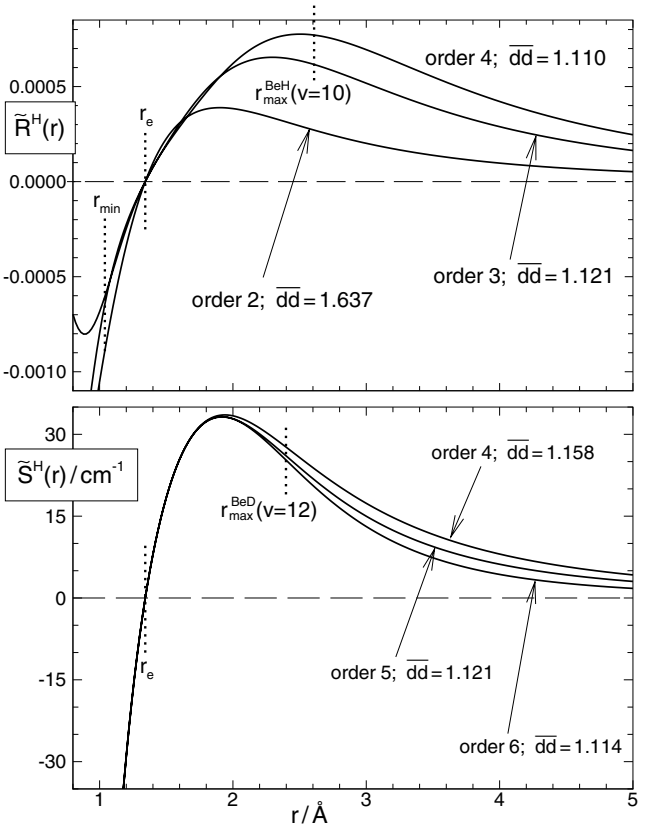

Fig. 3. Lower: potential energy BOB function for BeH. Upper: centrifugal BOB function for BeH.

er end of the range over which data are available for both isotopologues, the outer turning point of the highest observed level of BeD, $r_{\max}^{\mathrm{BeD}}(v=12)$; this attests to the physical significance of our $\tilde{S}_{\mathrm{ad}}^{\mathrm{H}}(r)$ functions inside this range. Similarly, the fact that the order 3 and 4 polynomials for $\tilde{R}_{\mathrm{na}}^{\mathrm{H}}(r)$ begin to differ significantly at distances smaller that the outer turning point of the highest observed level of BeH, $r_{\max}^{\mathrm{BeH}}(v=10)$, reflects the fact that data involving the highest observed vibrational levels are only available for relatively low J values. This model dependence indicates that our $\tilde{R}_{\mathrm{na}}^{\mathrm{H}}(r)$ function is probably only well determined for $r \lesssim 2$ Å.

We also note that the actual fitted value (before rounding) of our dissociation energy, 17591.4(±3.9) cm^{-1}, had an unrealistically small estimated uncertainty, and differs from the 1975 experimental value [7] of 17426(± 100) cm^{-1} by more than its estimated uncertainty. The former is a common problem in direct-potential-fit analyses, and reflects the fact that the largest source of uncertainty in such fits is model dependence, an effect that is quite difficult to estimate. Our ad hoc estimate of the uncertainty in this quantity is the ±200 cm^{-1} value quoted in Table 4.

3.3. Treatment of the $A^2\Pi$ and $C^2\Sigma^+$ states

Due to the strong interaction between the $A^2\Pi$ and $C^2\Sigma^+$ states [4], perturbations in the rotational structure of many of the $A-X$ and $C-X$ bands make it impossible to apply to those upper states simple single-state models such as that applied to the ground state. With the properties of the ground state defined by band constants generated from the parameters of Table 2, attempts were made to de-perturb the upper state levels by simultaneously fitting to the $A-X$ and $C-X$ data while allowing for additional interaction matrix elements between the A and C states, as was done in an earlier paper [4]. Unfortunately, the interaction only affects a few levels at each crossing point between the rotational series for A and C state vibrational levels, and in most cases, the perturbed levels are only observed for the $A-X$ bands. These proved insufficient to allow us to determine the interaction parameters reliably, so our attempt to perform a global deperturbation analysis was unsuccessful.

The best we were able to do was to selectively omit (or deweight) transitions involving heavily perturbed upper-state levels, and determine a separate set of band constants (G_v, B_v, D_v, ...) for each vibrational level of each isotopologue from conventional least-square analyses of the $A-X$ and $C-X$ systems together. In these fits, the ground-state band constants were fixed at those derived from the Dunham-type parameter set of Table 2, and are available from the authors or from the Journal's data archive [25]. The usual Hamiltonian matrix elements for $^2\Sigma$ and $^2\Pi$ states [37,38] were used to reduce the experimental data to molecular constants. For the $A^2\Pi$ state, higher-order elements related to the Λ-doubling constants q_{H} and q_{L} were calculated by matrix multiplication, and the higher-order "mechanical" rotational constants L_v, M_v, and N_v were also required. The resulting molecular constants for the $A^2\Pi$ and $C^2\Sigma^+$ states of the isotopologues of BeH are presented in Tables 5–8, and the complete line list, together with the "Observed − Calculated" values resulting from these fits are available from the Journal's data archive [25]. The principal spectroscopic constants for the $A^2\Pi$ and $C^2\Sigma^+$ states of BeH determined from fits to the band constants of Tables 5 and 8 are shown in Table 9. Due to the strong perturbations of the $v=5$ and 6 levels of $A^2\Pi$ state of BeH, only constants for its lowest five levels ($v=0$–4) were used in these fits. These constants were used to generate the RKR potentials for these states shown in Fig. 2.

4. Conclusion and discussion

Comprehensive combined-isotopologue data analyses of all available infrared and electronic data involving the

Table 5
Recommended band constants for the $A^2\Pi$ state of BeH, in units cm^{-1}

v	0	1	2	3	4	5	6
T_v	21052.2688 (16)	23059.0320 (12)	24981.3443 (18)	26816.8072 (26)	28562.3197 (41)	30213.8036 (26)	31766.272 (50)
B_v	10.302467 (23)	9.970044 (27)	9.630745 (42)	9.281491 (95)	8.91920 (14)	8.540147 (12)	8.13845 (38)
$10^3\times D_v$	1.044926 (85)	1.040092 (91)	1.04000 (15)	1.04383 (58)	1.05216 (71)	1.07804 (93)	1.1048 (16)
$10^8\times H_v$	9.530 (12)	9.204 (10)	9.040 (19)	8.831 (12)	7.946 (80)	7.87 (14)	9.01 (22)
$10^{11}\times L_v$	−1.1228 (71)	−1.1341 (48)	−1.4007 (79)	−1.997 (84)	[−2.1]	[−2.6]	[−3.2]
$10^{16}\times M_v$	3.6 (15)	−0.92 (17)					
A	2.198 (15)	2.1572 (95)	2.165 (12)	2.190 (16)	2.163 (23)	[2.16]	[2.15]
$10^3\times\gamma$	−8.65 (41)	−6.41 (25)	−6.48 (22)	−7.00 (48)	−6.10 (59)	−4.87 (38)	−7.22 (43)
$10^6\times\gamma_D$	6.9 (13)[a]	5.00 (37)	4.70 (27)	5.2 (10)	[5.0]	[5.0]	[5.0]
$10^2\times q$	1.4003 (19)	1.3506 (38)	1.2709 (56)	1.221 (16)	1.156 (26)	0.996 (14)	0.752 (44)
$10^6\times q_D$	−6.102 (58)	−6.74 (14)	−6.91 (23)	−8.99 (10)	−15.3 (12)	−29.34 (81)	−35.6 (11)
$10^9\times q_H$	1.282 (54)	1.93 (15)	2.26 (30)	4.0 (22)	15.3 (15)	[40.]	[100.]
$10^{13}\times q_L$	−2.63 (16)	−6.28 (55)	−12.7 (13)	−28. (15)	[−110.]	[−200.]	[−400.]

Numbers in parentheses one standard error uncertainty in the last digits shown, while parameter values in square brackets were held constant in the fit. Values of T_v are expressed relative to the extrapolated $v=-1/2$ energy for BeH in the $X^2\Sigma^+$ state.

[a] For $v=0$ the fit also required the two additional parameters $\gamma_{\mathrm{H}}=9.6(15)\times10^{-9}$ and $\gamma_{\mathrm{L}}=-1.250(74)\times10^{-11}$.

Table 6
Recommended band constants for the $A^2\Pi$ state of BeD, in units cm^{-1}; as in Table 5

v	0	1	2	3	4	5	6
T_v	20797.5504 (14)	22302.8104 (15)	23761.9908 (20)	25174.2415 (23)	26538.5185 (32)	27853.5814 (56)	29117.9376 (76)
B_v	5.696002 (12)	5.560807 (17)	5.423728 (23)	5.284250 (43)	5.141936 (41)	4.99590 (36)	4.84473 (13)
$10^4 D_v$	3.17121 (27)	3.15871 (45)	3.15125 (55)	3.15009 (77)	3.1617 (12)	3.18001 (29)	3.19052 (55)
$10^8 H_v$	1.6089 (23)	1.5754 (43)	1.5350 (46)	1.4881 (72)	1.482 (12)	1.409 (37)	1.148 (62)
$10^{12} L_v$	−1.0401 (88)[a]	−1.068 (18)	−1.135 (13)	−1.267 (22)	−1.624 (38)	−1.91 (16)	[−2.0]
A	2.190 (13)	2.228 (16)	2.278 (27)	2.347 (29)	2.470 (51)	2.661 (76)	2.636 (65)
$10^3 \gamma$	−7.07 (25)	−6.51 (38)	−6.58 (38)	−8.18 (46)	-9.23 (63)	−11.79 (49)	−14.22 (52)
$10^6 \gamma_D$	8.59 (45)	6.54 (80)	6.33 (67)	9.47 (87)	11.9 (13)	16.85 (59)	[30.]
$10^9 \gamma_H$	−3.62 (22)	−2.19 (45)	−1.85 (28)	−3.26 (41)	-4.71 (67)	[−7.]	[−11.]
$10^3 q$	4.1916 (70)	4.053 (11)	3.891 (18)	3.717 (15)	3.557 (18)	3.258 (44)	[2.4]
$10^7 q_D$	−8.783 (89)	−8.72 (15)	−9.01 (34)	−9.28 (15)	-10.34 (23)	[−11.]	[−12.]
$10^{11} q_H$	4.15 (26)	2.93 (52)	2.8 (15)	[4.]	[4.]	[4.]	[4.]

Values of T_v are expressed relative to the extrapolated $v = -1/2$ energy for BeH in the $X^2\Sigma^+$ state.
[a] For $v = 0$ the fit also required the additional parameter $M_v = 1.93(12) \times 10^{-17}$.

Table 7
Recommended band constants for the $A^2\Pi$ state of BeT, in units cm^{-1}; as in Table 5

v	0	1	2	3
T_v	20689.046 (18)	21979.490 (44)	23236.512 (65)	24459.371 (50)
B_v	4.15531 (13)	4.07215 (61)	3.9893 (10)	3.90477 (74)
$10^4 D_v$	1.6520 (26)	1.670 (22)	1.757 (43)	1.760 (29)
$10^9 H_v$	3.57 (14)	7.5 (23)	16.7 (51)	12.6 (31)
A	[2.0]	[2.0]	[2.0]	[2.0]
$10^3 \gamma$	−1.31 (20)	−1.73 (39)	−2.27 (59)	−1.82 (50)
$10^5 \gamma_D$	1.93 (45)	2.83 (87)	4.55 (16)	3.5 (13)
$10^9 \gamma_H$	−7.2 (23)	[−7.2]	[−7.2]	[−7.2]
$10^3 q$	2.87 (16)	2.54 (43)	3.05 (48)	2.37 (44)
$10^6 q_D$	−3.44 (42)	−4.1 (12)	−4.7 (11)	−2.1 (11)
$10^{11} q_H$	3.05 (25)	[3.1]	[3.1]	[3.1]

Values of T_v are expressed relative to the extrapolated $v = -1/2$ energy for BeH in the $X^2\Sigma^+$ state.

Table 8
Recommended band constants for the $C^2\Sigma^+$ state of BeH and BeD, in units cm^{-1}; as in Table 5

	v	T_v	B_v	$10^4 D_v$	$10^8 H_v$	$10^{12} L_v$
BeH	0	31466.464 (16)	3.52211 (16)	1.839 (12)	2.15 (11)	—
	1	32457.063 (22)	3.52279 (58)	1.3734 (40)	[2.0]	—
	2	33401.088 (50)	3.4946 (15)	2.075 (85)	[2.0]	—
BeD	0	31339.292 (30)	1.94162 (31)	0.5579 (84)	0.656 (82)	−1.48 (25)

Values of T_v are expressed relative to the extrapolated $v = -1/2$ energy for BeH in the $X^2\Sigma^+$ state.

ground $X^2\Sigma^+$ state have been performed using both a traditional "parameter-fit" approach based on Dunham-type level energy expression, and direct-potential-fit methods. Both approaches represented the available data approximately within the estimated experimental uncertainties: the dimensionless root mean square deviation was $\overline{dd} = 1.01$ for the Dunham-type analysis and 1.12 for the DPF analysis. The DPF analysis required only 19 free parameters to represent the 2821 data (1308 for BeH, 1333 for BeD, and 180 for BeT), while the unconstrained Dunham-type analysis required 51 free parameters, and the former approach is expected to give more realistic predictions for levels in the region beyond the range of the existing data (Table 10).

The $X^2\Sigma^+$ state of BeH has long been an intriguing system because of the question of whether or not there exists either a potential energy barrier or irregular behaviour in the form of multiple inflection points in the long-range region. This possibility was noted, and then discounted in early electronic structure studied of this system [9,10], but was given new impetus by Colin et al. [4], based on analyses of the cutoff of rotational progressions, presumably due to tunneling predissociation. A number of subsequent ab initio studies have examined this point, and they tended to find that a barrier would appear in preliminary calculations, but disappear as the basis set size was increased or the quality of calculation improved in other ways [11,12,14]. Cooper [11] also

Table 9
Principal molecular constants for the $A^2\Pi$ and $C^2\Sigma^+$ states of BeH, all with units cm^{-1}

constant	$A^2\Pi$	$C^2\Sigma^+$
$\mathfrak{D}_e$	19389 (200)	8453 (200)
$T_v = -1/2$	20018.16 (20)	30953.94
$Y_{1,0}$	2088.38 (36)	1036.59
$Y_{2,0}$	−40.09 (17)	−23.09
$Y_{3,0}$	−0.458 (43)	...
$Y_{0,1}$	10.46715 (6)	3.511
$Y_{1,1}$	−0.32873 (11)	0.0296
$10^4 Y_{2,1}$	−9.83 (51)	−144.3
$10^4 Y_{3,1}$	−5.38 (68)	...

For the $A^2\Pi$ state the numbers in parentheses represent 95% confidence limit uncertainties in the last digits shown; for the $C^2\Sigma^+$ state no uncertainties are given, since the fit had no degrees of freedom. The values of T_v are expressed relative to the extrapolated $v = -1/2$ energy for the $X^2\Sigma^+$ state.

Table 10
Predicted band constants for unobserved vibrational levels of the $X^2\Sigma^+$ state of BeH and BeD, in units cm^{-1}

	v	T_v	B_v	$10^4 D_v$	$10^6 H_v$
BeH	11	17424.3	4.0486	55.5	−15.2
BeD	13	16291.1	3.3907	5.74	−0.129
	14	16955.4	2.9501	8.23	−0.384
	15	17433.5	2.2309	16.8	−2.47

Values of T_v are expressed relative to the extrapolated $v = -1/2$ energy for $X^2\Sigma^+$ state BeH.

reported simulations which suggested that the rotational cutoff behaviour described by Colin et al. [4] might be an artifact due to uncertainties in the extrapolation of such cutoffs to the $J = 0$ limit. On the other hand, some of the most recent calculations on these systems yields potentials which have either a barrier or multiple inflection points in the 3–5 Å region [15,17,18,39].

The present work does not attempt to resolve the question of whether or not this potential function has a barrier or multiple inflection points in the outer well region. However, the ambiguity raised by this question influenced our choice of potential energy function form. In particular, if there was no irregular behaviour, the outer wall of the potential function would have one inflection point and eventually approach its asymptote with the limiting $V(r) \simeq \mathfrak{D} - C_6/r^6$ behaviour expected for a pair of separating S-state atoms. If this were the case, it would have been more appropriate to represent the potential by the "Morse/Lennard-Jones" (MLJ) model of [40] and [41], which explicitly incorporates that long-range behaviour. On the other hand, if a potential barrier does exist, the vibrational level energies would be expected to converge to a limit which would correspond (approximately) to the energy at the maximum of that barrier. Since a potential function would approach such a limit much more rapidly than an inverse power of r, the exponential long-range cutoff of an EMO potential function would provide a more realistic model for this situation. Moreover, even for potentials with no irregular outer-wall behaviour, if the experimental data region does not extend close to the region near dissociation where the inverse-power long-range behaviour becomes dominant, the simpler EMO potential function model might be considered more appropriate. Because of this ambiguity, the ground-state dissociation energy was treated as a free parameter in our analysis, and not fixed at the estimate of $\mathfrak{D}_e = 17426(\pm 100)\ cm^{-1}$ reported in [7]. The difference between this value and the $17590(\pm 200)\ cm^{-1}$ characterizing our recommended potential function is an indication of the current level of uncertainty regarding this well depth.

Finally, we note that our potential function for the $X^2\Sigma^+$ state supports one more vibrational level that has been observed for BeH ($v = 11$) and three more than have been observed for BeD ($v = 13$–15). The energies and leading rotational constants for those levels are listed in Table 10. Note, however, that the uncertainty in the dissociation energy and the precise nature of the potential function extrapolation beyond the data region means that these predictions are not expected to be definitive.

Acknowledgments

We are pleased to thank the Belgian National Fund for Scientific Research (FRFC Convention), the Communauté française of Belgium (Actions de Recherche Concertées), and the Natural Sciences and Engineering Research Council of Canada for financial support of this research.

Appendix A. Supplementary data

Supplementary data for this article are available on ScienceDirect (www.sciencedirect.com) and as part of the Ohio State University Molecular Spectroscopy Archives (http://msa.lib.ohio-state.edu/jmsa_hp.htm).

References

[1] A. Shayesteh, K. Tereszchuk, P.F. Bernath, R. Colin, J. Chem. Phys. 118 (2003) 1158.
[2] C. Focsa, S. Firth, P.F. Bernath, R. Colin, J. Chem. Phys. 109 (1998) 5795.
[3] C. Focsa, P.F. Bernath, R. Mitzner, R. Colin, J. Mol. Spectrosc. 192 (1998) 348.
[4] R. Colin, C. Drèze, M. Steinhauer, Can. J. Phys. 61 (1983) 641.
[5] R. Horne, R. Colin, Bull. Soc. Chim. Belgium 81 (1972) 93.
[6] D.R.C. De Greef, J. Mol. Spectrosc. 53 (1974) 455.
[7] R. Colin, D. De Greef, Can. J. Phys. 53 (1975) 2142.
[8] C. Clerbaux, R. Colin, Mol. Phys. 72 (1991) 471.
[9] P.S. Bagus, C.M. Moser, P. Goethals, G. Verhaegen, J. Chem. Phys. 58 (1973) 1886.
[10] G. Gerratt, M. Raimondi, Proc. Roy. Soc. (London) A 371 (1980) 525.
[11] D. Cooper, J. Chem. Phys. 80 (1984) 1961.
[12] M. Larsson, J. Chem. Phys. 81 (1984) 6409.
[13] M. Larsson, Physica Scripta 32 (1985) 97.
[14] C. Henriet, G. Verhaegen, Physica Scripta 33 (1986) 299.
[15] X. Li, J. Paldus, J. Chem. Phys. 102 (1995) 2013.

[16] F.B.C. Machado, O. Roberto-Neto, F.R. Ornellas, Chem. Phys. Lett. 284 (1998) 293.
[17] I.D. Petsalakis, D. Papadopoulos, G. Theodorakopoulos, R.J. Buenker, J. Phys. B: Atoms. Mol. Opt. Phys. 32 (1999) 3225.
[18] H. Meissner, J. Paldus, J. Chem. Phys. 113 (2000) 2622.
[19] R.J. Le Roy, J. Mol. Spectrosc. 191 (1998) 223.
[20] R.J. Le Roy, J. Mol. Spectrosc. 194 (1999) 189.
[21] R.J. Le Roy, Y. Huang, J. Mol. Struct. (Theochem) 591 (2002) 175.
[22] DPotFit 1.0, A Computer Program for fitting Diatomic Molecule Spectra to Potential Energy Functions, University of Waterloo Chemical Physics Research Report CP-662 (2005); see the "computer programs" link at <http://leroy.uwaterloo.ca>.
[23] J.M. Brown, A. Carrington, Rotational Spectroscopy of Diatomic Molecules, Cambridge University Press, Cambridge UK, 2003.
[24] R.J. Le Roy, DParFit 3.3: A Computer Program for Fitting Multi-Isotopologue Diatomic Molecule Spectra, University of Waterloo Chemical Physics Research Report CP-660 (2005); see the "computer programs" link at <http://leroy.uwaterloo.ca>.
[25] Supplementary data for this article consisting of complete ASCII listings of the parameters of Table 2 and the band constants generated from them, and of the experimental data used in the X-state analysis, and a PDF file listing the data used in the A- and C-state analyses, are available on ScienceDirect (www.sciencedirect.com) and as part of the Ohio State University Molecular Spectroscopy Archive (http://msa.lib.ohio-state.edu/jmsa_hp.htm).
[26] (a) R. Rydberg, Z. Physik 73 (1931) 376;
(b) O. Klein, Z. Physik 76 (1932) 226;
(c) R. Rydberg, Z. Physik 80 (1933) 514;
(d) A.L.G. Rees, Proc. Phys. Soc. (London) 59 (1947) 998.
[27] R.J. Le Roy, RKR1 2.0: A Computer Program Implementing the First-Order RKR Method for Determining Diatomic Molecule Potential Energy Curves, University of Waterloo Chemical Physics Research Report CP-657 (2003); see the "computer programs" link at <http://leroy.uwaterloo.ca>.
[28] J.K.G. Watson, J. Mol. Spectrosc. 80 (1980) 411.
[29] J.K.G. Watson, J. Mol. Spectrosc. 223 (2004) 39.
[30] J.F. Ogilvie, J. Phys. B: At. Mol. Opt. Phys. 27 (1994) 47.
[31] Y. Huang, R.J. Le Roy, J. Chem. Phys. 119 (2003) 7398.
[32] The notation for BOB correction functions used here differs that of our earlier work [20,21] in an effort to make it more consistent with that used by others [28,30,29] and to avoid confusion with the "q" notation commonly used for Λ–doubling parameters. Note, however, that our use of the reference-isotopomer convention of [20] means that the present $\tilde{S}^A_{\rm ad}(r)$ differs from Watson's [28,29] $\tilde{S}^A(r)$ by the factor $\Delta M^{(\alpha)}_A/m_{\rm e}$ and that our $\tilde{R}^A_{\rm na}(r)$ differs from his $\tilde{R}^A(r)$ by the factor $M^{(1)}_A/m_{\rm e}$, where $m_{\rm e}$ is the electron mass.
[33] R.J. Le Roy, D.R.T. Appadoo, K. Anderson, A. Shayesteh, I.E. Gordon, P.F. Bernath, J. Chem. Phys. 123 (2005) 1–11.
[34] A.A. Šurkus, R.J. Rakauskas, A.B. Bolotin, Chem. Phys. Lett. 105 (1984) 291.
[35] Y. Huang, Determining Analytical Potential Energy Functions of Diatomic Molecules by Direct Fitting, M.Sc. Thesis, Department of Chemistry, University of Waterloo, 2001.
[36] R.J. Le Roy, LEVEL 7.7: A Computer Program for Solving the Radial Schrödinger Equation for Bound and Quasibound Levels, University of Waterloo Chemical Physics Research Report CP-661 (2005); see the "computer programs" link at <http://leroy.uwaterloo.ca>.
[37] C. Amiot, J.-P. Maillard, J. Chauville, J. Mol. Spectrosc. 87 (1981) 196.
[38] M. Douay, S.A. Rogers, P.F. Bernath, Mol. Phys. 64 (1988) 425.
[39] X. Li and J. Paldus, private communication (2005).
[40] P.G. Hajigeorgiou, R.J. Le Roy, in: 49th Ohio State University International Symposium on Molecular Spectroscopy (Ohio State University, Columbus, Ohio, 1994), paper WE04.
[41] P.G. Hajigeorgiou, R.J. Le Roy, J. Chem. Phys. 112 (2000) 3949.